Assessing Heat Flow Patterns in Basement Walls with Exterior Insulation

Michael C. Swinton, P.E. *Member ASHRAE*
Wahid Maref, Ph. D.
Mark Bomberg, Ph. D.
M. Kumar Kumaran, Ph. D.
Nicole Normandin

ABSTRACT

Most of the studies on the thermal performance of basement construction systems have focused on modeling. There has been a lack of detailed monitored performance data to substantiate the models. Therefore, a joint research project of industry and the Institute for Research in Construction was initiated to assess the in-situ thermal performance of a number of insulation products used as exterior basement insulation. The effect of two-year monitoring provided an opportunity to analyze, in detail, the heat flow patterns in two experimental walls, each having eight insulation specimens instrumented side by side.

This paper presents key findings on both the experimental and analytical side. A number of analytic tools (two-dimensional and three-dimensional analyses) were developed to interpret the temperature fields in detail. As a result, a clearer picture of two- and three-dimensional heat flow patterns within the basement walls was developed. The analysis provided in this paper deals with heat flow through the exterior insulation below grade, as well as vertical and lateral components of heat loss and thermal storage effects in the concrete wall.

With this information, the authors can differentiate between the thermal performance of the wall system and that of the insulation materials themselves.

INTRODUCTION

In Canada, the basement has become a part of the habitable living space. Combined with requirements in energy efficiency, this has prompted the development of insulated basement systems. Some of these systems use thermal insulation on the exterior of the basement wall. In addition to reducing heat loss, external insulation may also have a significant effect on the moisture performance and durability of the basement envelope system.

The need to protect the foundation from the below-grade environment is not a new concept (Crocker 1961; Elmorth and Holglund 1971; Crocker 1974; Bomberg 1978; Timusk 1981; Hutcheon 1963). Over the years, new products and systems have been introduced to perform this function. How these new materials actually perform and whether or not they can meet the performance requirements for basements were key issues addressed by those responsible for developing regulations governing their use in Canadian construction.

Previous papers by Sterling (1986) and Nelson (1989) were intended to establish the suitability of insulation products for below-grade application, mainly through the laboratory measurements of properties after exposure. Little information was available on the in situ thermal performance and on the performance of insulation products exposed unprotected in below-grade applications.

In this context, the Canadian thermal insulation industry, working together with the National Research Council, decided to revisit (see Tao et al. 1980; Bomberg 1980) the design and performance of external insulation basement systems (EIBS).

OBJECTIVES

This research project was undertaken to determine the effect of the below-grade environment on the in situ thermal

Michael C. Swinton is a senior research officer, **Wahid Maref** is a research officer, **M. Kumar Kumaran** is a senior research officer, and **Nicole Normandin** is a technical officer at the Institute for Research in Construction, National Research Council Canada (IRC/NRCC), Ottawa, Ontario, Canada. **Mark T. Bomberg** was a senior research officer at the Institute for Research in Construction, but is now affiliated with Concordia University, Montreal.

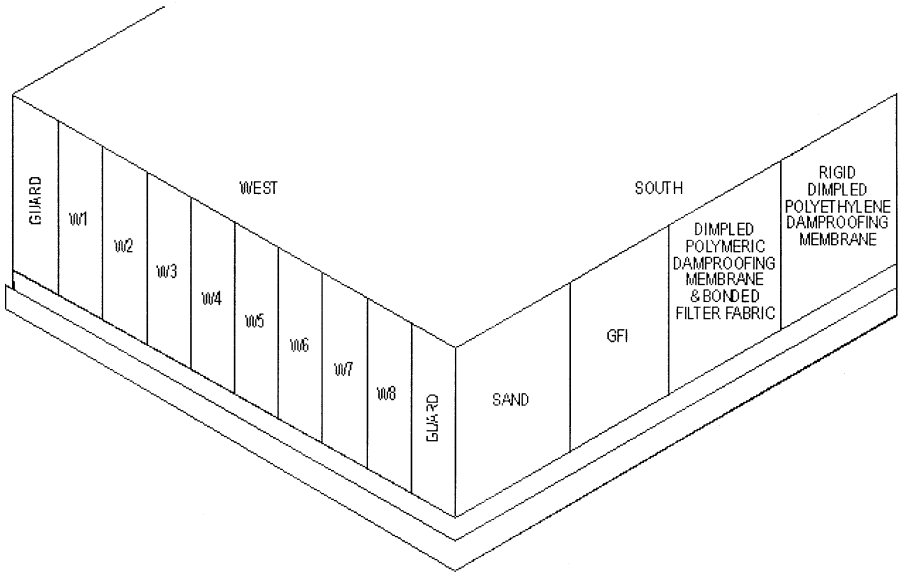

Figure 1 *Schematic of placement of specimens on the west wall.*

performance of exterior basement insulation systems. It involved a number of material and system issues. Material considerations included the selection of existing and new thermal insulation products (under development). These products were placed side-by-side on the basement wall to create virtual test compartments. The insulation was exposed to the Ottawa climate, including below-grade conditions, over a two-and-a-half-year period from October 1995 to June 1998. Over this period, ten expanded polystyrene (EPS), two spray polyurethane foam (SPF), two mineral-fiber insulation (MFI), and two glass-fiber insulation (GFI) specimens were placed on the exterior of the basement wall in the experimental building located on the NRC campus in Ottawa.

RESEARCH APPROACH

To evaluate performance of exterior basement insulation, different materials were installed on the exterior surface of concrete basement walls. Eight test specimens were placed side-by-side on each of two basement walls (east and west) insulating a whole wall with approximately 2.99 in. (76 mm) thick and 7.87 ft (2.4 m) high specimens. The full width of each wall was 31 ft (9.5 m). Each panel was either 2 ft (610 mm) wide (EPS) or 4 ft (1220 mm) wide (all other specimens). On the interior of the wall, a 0.98 in. (25 mm) layer of expanded polystyrene (EPS) board was installed over the entire surface (full height and width of the basement wall) in order to more easily calibrate and measure the heat flux at the interior surface. At three vertical locations on each test wall, cutouts were made and calibrated EPS specimens, with identical thickness, were tightly inserted. These specimens were used for determination of transient heat flux entering the wall (Bomberg et al. 1994).

Thermocouples were placed at the boundary surfaces, as well as the interfaces of each layer in the wall, in an array consisting of 16 points per tested compartment. All sensors placed on the west wall are shown in Figure 2. The extremities of the control volume for analysis of the experimental results are defined by the uppermost and lowermost thermocouples shown in Figure 2.

The parameters monitored in the EIBS are

1. surface temperatures on both sides of the calibrated EPS specimen, the concrete, and the insulation test specimens,
2. heat flux across the calibrated EPS specimens,
3. soil temperatures from 3.28 ft (1 m) to 6.56 ft (2 m) away from the specimens and at five depths,
4. interior basement air temperature (average of four readings, each located roughly in the middle of each quadrant of the basement),
5. exterior air temperature (at north face, shielded from sun), and
6. relative humidity (RH) and other parameters of indoor and outdoor environments.

The instrumentation package consisted of approximately 145 thermocouples, 2 humidity sensors, 21 calibrated insulation specimens (heat flux transducers), 4 junction boxes, and a data acquisition unit operated by a computer.

Indoor and Outdoor Air Temperature Profiles

The indoor and outdoor air temperature profiles over the two heating seasons are shown in Figure 3. Data were recorded every half-hour. Every eighth reading (i.e., every four hours) was plotted.

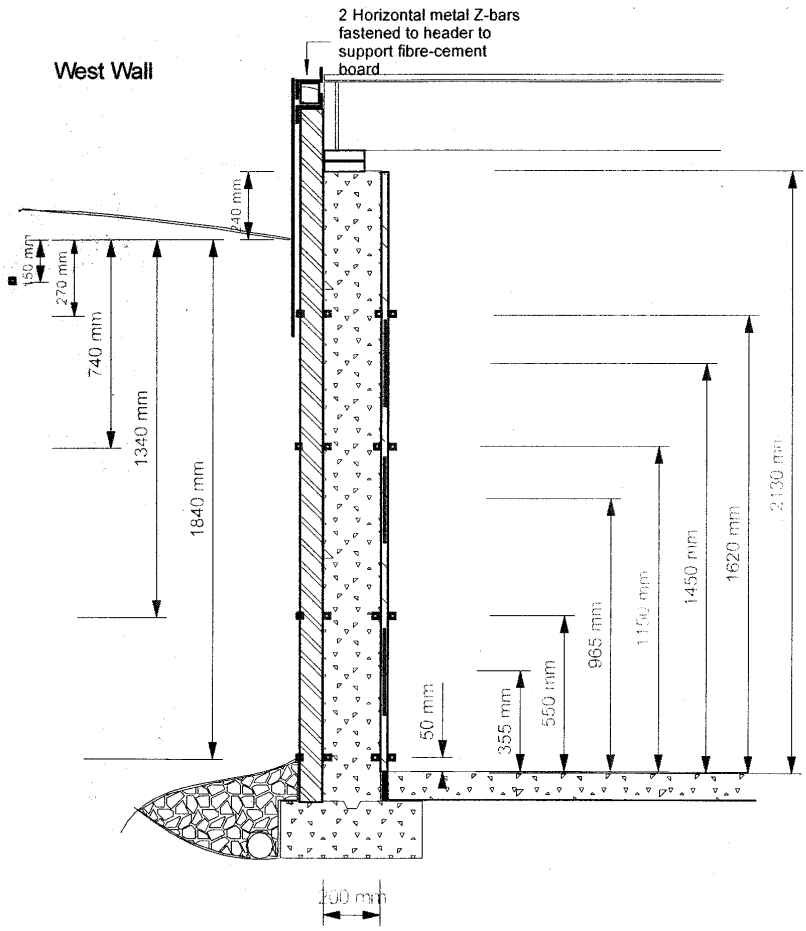

Figure 2 *Thermocouples (shown as square dots) and calibrated insulation specimens (shown as sections of the calibrated layer, dimensions are to the center of the section) on the west wall.*

The indoor basement air temperature was held relatively steady at 73.4°F (23°C), with some loss of control experienced in the shoulder seasons. The switch from heating to air conditioning on the heat pump was manual, resulting in slight overheating of the basement on warm days in the spring and the fall when the heat pump was set to heating.

The outdoor temperatures show both the diurnal variations and seasonal trends following a rough sine wave. The winter of 1997 featured one very cold night only, with temperatures dipping to about –22°F (–30°C). Neither winter showed a sustained cold snap—each very cold evening was often followed by a thaw (temperatures climbing above 32°F [0°C]). The degree-days over the two years of monitoring were calculated to be about 8% below average for Ottawa. This unexpected weather pattern may have resulted in low frost penetration, as documented further in the report.

Soil Temperatures

Soil temperatures were measured at a distance of 6.56 ft (2 m) from the wall. The results for the instrument set nearest specimen W6 are shown for three depths in Figure 4. These were measured at 5.91 in. (150 mm), 29.1 in. (740 mm), and 72.44 in. (1840 mm) below grade, over a two-year period. The sensors nearest to the soil surface showed the greatest variation from summer to winter, and diurnal effects could be observed. No diurnal effects could be seen at the two lower depths. The temperatures at the lowest depth approximated a sine wave each year.

It should be noted that in both winters, the frost penetrated approximately 5.91 in. (150 mm). The frost depth temporarily reached 10.63 in. (270 mm) in the second winter (not shown in graph). Deep snow cover and repeated thaws in both heating seasons may be the cause of shallow frost penetration. An

independent temperature measurement in the second winter, 32.81 ft (10 m) from the house, showed the same result. This indicates that there was an undetectable effect because of basement heat loss on the soil temperature at 6.56 ft (2 m) from the house.

Temperatures through the Wall System

Figure 5 shows measured temperatures of indoor air, calibrated EPS layer, concrete, test specimen, and soil surface in the "mid-position" of the wall over a period of two years. The spikes in the interface between soil and the EIBS correspond to thaw periods or episodes of heavy rainfall. Observe that

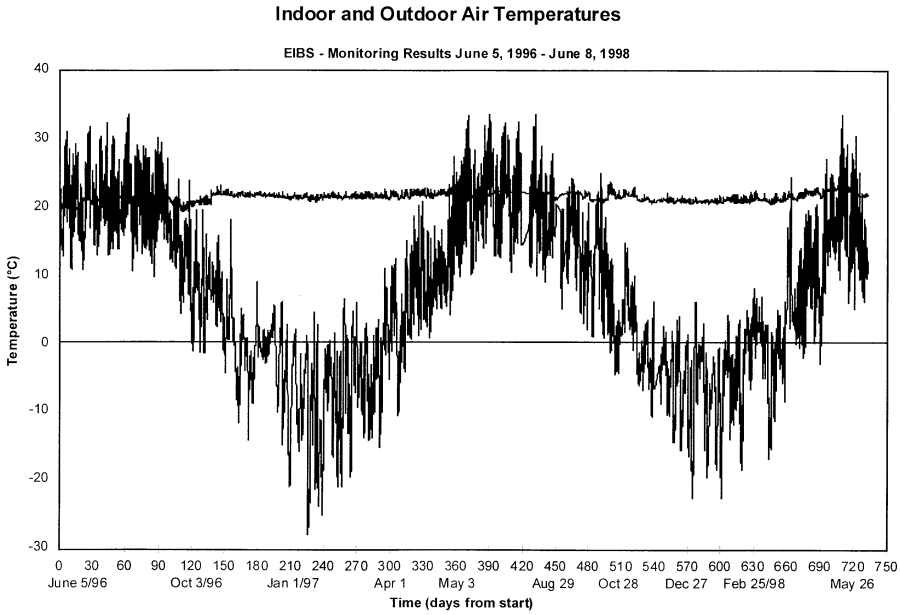

Figure 3 *Temperatures across the W6 specimen measured in the mid-height position.*

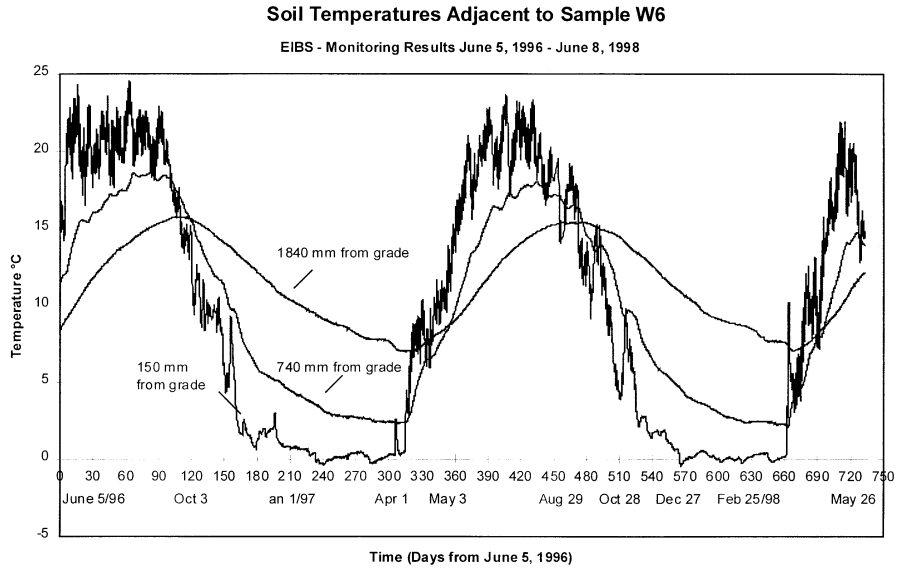

Figure 4 *Indoor and outdoor temperature profile over the monitoring period.*

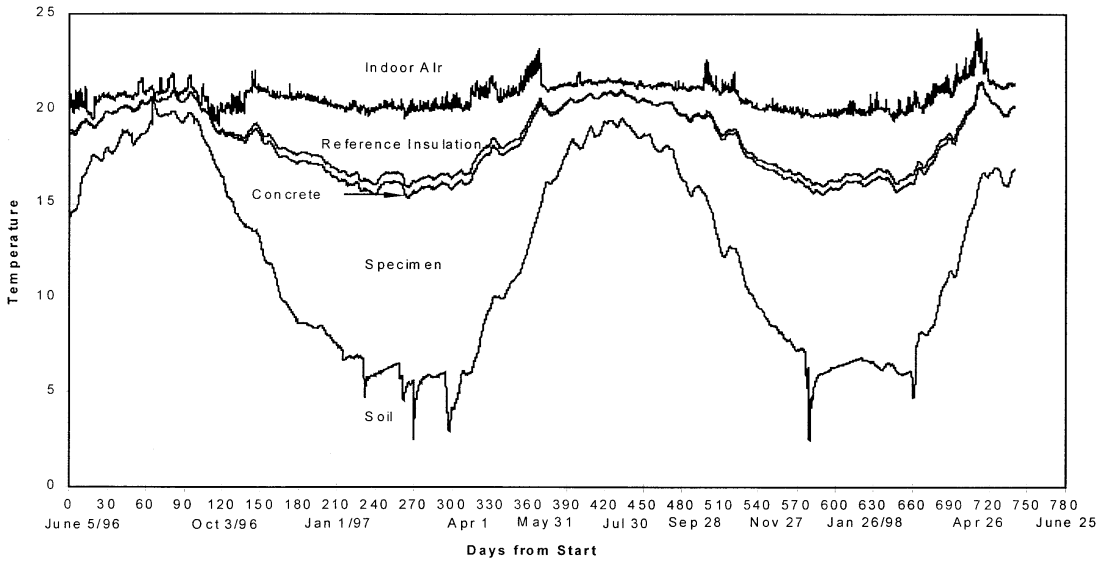

Figure 5 *Soil temperature profiles over the monitoring period.*

these effects do not appear to affect the temperature on the concrete surface (i.e., behind the external insulation).

Method to Measure Thermal Resistance In Situ

A test method, developed at NRC during a previous project (Muzychka 1992; Bomberg and Kumaran 1994), involves testing two insulating boards placed in contact with each other along the face of the material—a reference material whose thermal conductivity and specific heat are known as a function of temperature, and a test specimen whose thermal properties are unknown. Because of its comparative character, this method has been called a heat flow comparator (HFC). In this previous experiment involving roof insulation, the reference and tested specimens were placed in the exposure box representing a conventional roofing assembly. Thermocouples were placed on each surface of the test and reference materials to measure temperatures that were then used as the boundary conditions in the heat flow calculations.

The heat flux across the boundary surface between reference and test specimen is calculated using a numerical algorithm to solve the heat transfer equation through the reference material. Imposing the requirement of heat flux continuity at the contact boundary between test and reference materials, corresponding values of thermal conductivity and heat capacity of the test specimen are found with an iterative technique. This involves trial-and-error adjustment of the thermal properties of the test specimen until the continuity of heat flow is satisfied at the boundary between the materials. Surface resistance between the materials, if any, would be attributed to the thermal resistance of the test specimen. Performing these calculations for each subsequent data-averaging period will result in a set of thermal properties of the test material that, over the period of measurements, give the best match with its boundary conditions (temperatures and heat flux).

Since thermal conductivity of the specimen is a function of its temperature, the solution of the heat transfer equation is based on central finite difference calculations that include Kirchoff's potential function (integral of thermal conductivity over the range of temperature) and uses a Taylor's series to calculate heat flux through the surface. Subsequent developments improved the stability of the numerical solution and produced a user-friendly computer code that includes optimization routines. This method was documented and applied for determining the in situ thermal resistance of roof insulation (Bomberg and Kumaran 1994).

ANALYTICAL APPROACH

Examination of preliminary results highlighted difficulties in establishing the precision of thermal testing without addressing three-dimensional effects. For example, the temperature of the concrete behind the specimen with the highest nominal thermal resistance was higher than the temperature of the concrete behind neighboring specimens. Because of the high thermal conductivity of the concrete, it was clear that lateral heat flow needed to be accounted for—at least in the case with the higher thermal conductivity specimen.

To evaluate effects of lateral heat flow on the precision of the field measurements, a new task was added to the exterior insulation basement systems (EIBS) project, namely, the development of a three-dimensional model. The first question was then how to discretise the continuous equations to arrive at the system that was easy to solve with numerical techniques (see Maref et al. 2001).

Differences Between Two-Dimensional and Three-Dimensional Models

A two-dimensional finite difference analysis was developed by Swinton et al. (1999). This two-dimensional analysis consisted of calculating the horizontal (inside to outside) and vertical (bottom to top) heat fluxes through all material in the control volume. A finite difference technique was used to solve the heat transfer equations for each point of a nodal network within the control volume.

A more elaborate method was developed to assess the heat loss in the third dimension along the wall and to suggest what corrections were needed for the two-dimensional results (see Maref et al. 2001). The yearly difference between results obtained from two-dimensional and three-dimensional analyses was about 7% for the specimen with the highest thermal resistance. Other specimens showed closer agreement between two-dimensional and three-dimensional analyses (0% to 3% difference), since these specimens were flanked with specimens of similar thermal resistance.

Measured Vertical Heat Flux Profiles

Temperature differences across the thermally calibrated insulation layer at the inner face of the wall were calculated at four vertical locations with thermocouples and three vertical locations with heat flux meters as shown in Figure 2.

Example profiles of heat flux into the basement wall are shown in Figure 6. The smoothness or regularity of these curves attests to the fact that the seven vertical readings are consistent with another one. These weekly averaged heat flux profiles have the highest level of accuracy associated with them. Each heat flux meter reading is the result of the average of five junctions within the calibrated section to arrive at an average EMF reading.

Direction of the Heat Flow within the Wall

One of the key findings of the two-dimensional analysis was that the concrete layer, which was effectively sandwiched between the exterior insulation specimens and the interior calibrated insulation board, created a significant confounding effect in heat loss patterns. Because the soil temperatures are coldest near the ground surface in the wintertime, the concrete is also coldest in the upper portion of the wall, and heat tends to flow upward as well as outward. The resulting heat flux vectors calculated on an hourly basis are at an angle that is rarely 0º (i.e., rarely horizontal). The analysis was used to produce plots of these heat flux angles at various heights in the wall as a function of time over the monitoring period, as shown in Figure 7. It can be seen from the figure that the heat flux angle can vary from almost 60° in the upper wall to –60° at the bottom. Thus, a considerable portion of the heat flux, on the order of 20%, actually bypassed the insulation specimens below grade, going into the footing and up the wall above grade.

Lateral Heat Flow Calculation

Over the course of the two-dimensional analysis, it was noted that the temperature of the concrete (behind the specimens) differed from specimen to specimen. This raised the possibility that heat could flow through the concrete from one specimen to another, resulting in possible uncertainty in the orders of magnitude of performance assessed using the two-dimensional analysis.

In response to this, a detailed three-dimensional heat transfer analysis of both the east and west wall was undertaken. The same control volume used for the two-dimensional model (Swinton et al. 1999) was used for the three-dimensional analysis, but this was extended in the third dimension along the wall to encompass all specimens. The objective of this much more detailed analysis was to determine the order of magnitude of lateral heat flow in the concrete from one spec-

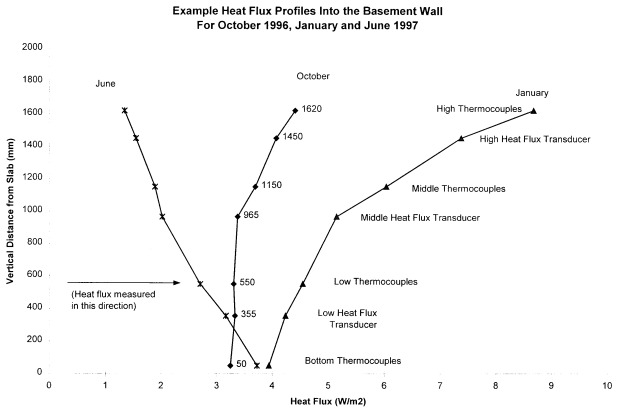

Figure 6 *Typical profiles of heat flux through the reference insulation at the inner face of the wall.*

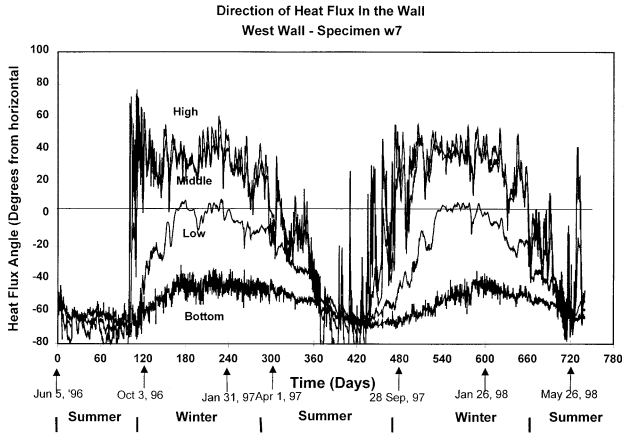

Figure 7 *Direction of heat flux in the wall over the monitoring period.*

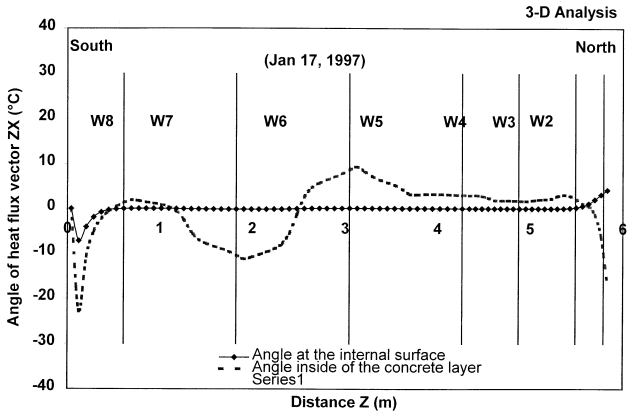

Figure 8 *Angle of heat flux vector calculated at the top position of the west wall. Positive sign indicates the lateral flow in the northward direction.*

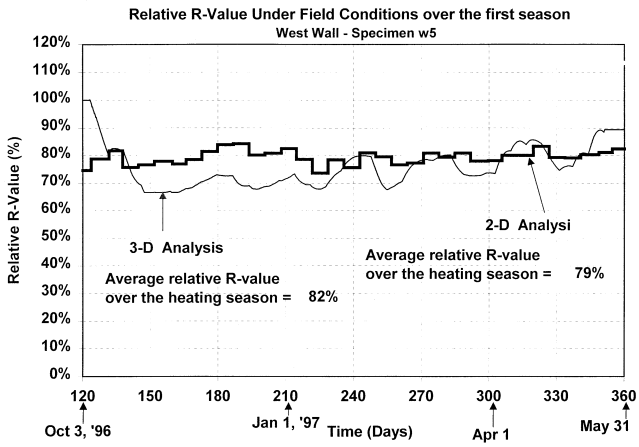

Figure 9 *Comparison of relative R-value under field conditions on the wet wall over the first heating season for specimen W5 (two-dimensional and three-dimensional).*

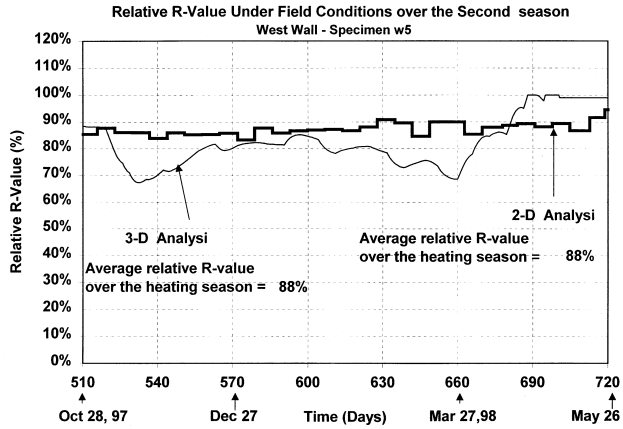

Figure 10 *Comparison of relative R-value under field conditions on the west wall over the second heating season for specimen W5 (two-dimensional and three-dimensional).*

imen to another, and to provide a correction on the two-dimensional results for in situ R-value of each specimen where needed.

To illustrate the results of this analysis, an example result is shown in Figure 8 for the west wall for a four-hour period on January 17, 1997. The angle between the actual heat flux vector and the normal direction is defined here as the heat flux angle (e.g., a zero angle denotes heat flux normal to the wall—no lateral heat flow). The heat flow angle is plotted for the "top" location (top of the control volume) in the concrete at one point in time. A positive angle means lateral heat flow toward one end of the wall, and a negative heat flow means lateral heat flow toward the other.

The significance of this diagram is as follows. If the flow angle in the concrete behind the test specimen is small and in the same direction, then the lateral heat flow has little effect on the results. This was the case for specimens W2, W3, W4, and W5. On the other hand, specimen W6 appears to have been affected by significant lateral heat flow. Starting at the center of the specimen, the heat flow on the south side is flowing south and the heat flow on the north side is flowing north. This is a lateral heat drain from the specimen, causing us to underestimate its thermal performance in the two-dimensional analysis. With this lateral flow, specimen W7 is gaining heat from W6. The two-dimensional analysis would underestimate the performance of W6 because the lateral heat loss that results in a lower concrete temperature is being interpreted as being due to more heat loss through the specimen. W8 appears to be influenced by an edge effect. This requires further investigation.

These lateral heat flows varied according to vertical position in the specimen and with time. The results were thus integrated over full height of the specimen and over each of two heating seasons. The three-dimensional analysis thus confirmed the order of magnitude of performance for specimens W2, W3, W4, W5, W7, and W8. The lateral heat flows affected specimen W6 in a significant way. The three-dimensional analysis showed generally better thermal performance of the W6 specimen than the two-dimensional analysis. Maref et al. (2001) have published details of the three-dimensional analysis.

Two-Dimensional and Three-Dimensional In Situ Thermal Resistance Comparisons

Figures 9 and 10 show the resulting thermal performance plots for the specimen W5 for the first heating season and the second heating season, respectively. Those figures show the comparison between the two-dimensional and the three-dimensional thermal performance. For the two-dimensional performance, the change in thermal resistance adjustment is

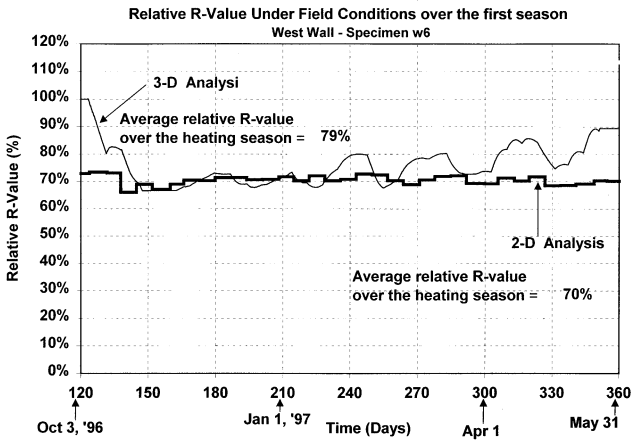

Figure 11 *Comparison of relative R-value under field conditions on the west wall over the first heating season for specimen W6 (two-dimensional and three-dimensional).*

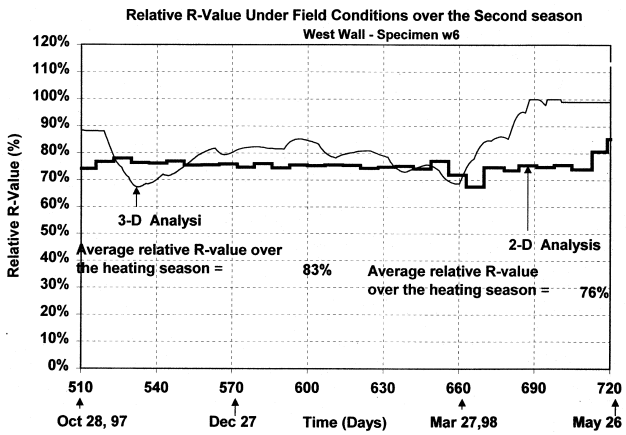

Figure 12 *Comparison of relative R-value under field conditions on the west wall over the second heating season for specimen W6 (two-dimensional and three-dimensional).*

shown on a weekly basis over the two heating seasons. The benchmark (100%) is the laboratory-determined value of thermal resistance of the specimen.

For the first heating season, the difference between the two-dimensional and the three-dimensional analyses on the average relative R-value is around 2%. For the second heating season, the difference is negligible.

Figure 8 shows that the flow angle in the concrete behind the specimen was small and in the same direction and the lateral heat flow had no effect on the results. It means that the two-dimensional plot gives the same analysis as the three-dimensional and for this reason the difference between the two-dimensional and the three-dimensional plot is small.

Figures 11 and 12 show the resulting thermal performance plots for specimen W6 for the first heating season and the second heating season, respectively. Those figures show the comparison between the two-dimensional and the three-dimensional thermal performance. For the two-dimensional, the change in thermal resistance adjustment is shown on a weekly basis over the two heating seasons.

The difference on the average relative R-value between the two-dimensional and the three-dimensional plot is around 9% for the first heating season and 7% for the second one. This means that for this specimen, the two-dimensional analysis underestimated the thermal performance during the two years by about 8%.

Observations on the results shown in Figures 9, 10, 11, and 12 are as follows:

- All specimens show relatively steady performance through the heating seasons.
- The second heating season shows equal or improved performance for all specimens.
- Major rain and thaw periods (shown in Figure 3) do not appear to significantly affect the thermal performance of the specimens during these episodes.

DISCUSSION

The following general observations are made as a result of these experiments and analysis.

1. Two-dimensional and three-dimensional analyses of the heat flow patterns in the wall were necessary to establish the role of the exterior thermal insulation in controlling heat transfer in the experimental wall.
2. The in situ tracking of thermal performance of the specimens indicated relatively stable thermal performance over the two years of monitoring. Nevertheless, there was an apparent slight improvement in specimen thermal performance in the second heating season. This correlated with dryer prevailing soil conditions in the second year. It also correlated with observed shrinking of the clay soil as it dried, likely resulting in less compression of the semi-rigid boards.
3. Based on the temperature profiles at the specimen/soil interface and corresponding visual observations of heavy rainfall or thaw periods that were recorded in daily logs, the specimens are apparently "handling" moving water at the specimen surface.

CONCLUDING REMARKS

For the conditions recorded over the two-year monitoring period in this experiment, the insulation specimens showed stable thermal performance in the soil, with each of the specimens showing only small variations from its average value. This performance was sustained even during major rainstorms and winter thaws when the effects of water movement were apparent at the outer face of the insulation specimens, contrary to expectations that the R-value would decline under such circumstances, especially if water were to move through the insulation.

A three-dimensional analysis was necessary to evaluate the effect of lateral heat flow in the concrete behind insulation products having different thermal resistance.

This study has shown the advantages given by the two-dimensional analysis and its limitations in evaluating the lateral heat flow. The three-dimensional analysis has given better assessment of this flow and of the long-term thermal resistance of the thermal insulating systems used in this study.

The three-dimensional analysis thus confirmed the order of magnitude of performance for specimens W5 and W6. The lateral heat flows affected specimen W6 in a significant way. The three-dimensional analysis showed better thermal performance of the W6 specimen than the two-dimensional analysis by about 9% in the first heating season and 7% in the second.

ACKNOWLEDGMENT

This project was sponsored by a consortium including Canadian Plastics Industry Association, Expanded Polystyrene Association of Canada, Canadian Urethane Foam Contractors Association, Owens Corning, Inc., and Roxul, Inc.

Deep gratitude and thanks are forwarded to Roger Marchand who installed the data acquisition system and John Lackey for his contribution in the experimental work.

REFERENCES

Bomberg, M.T. 1978. *Some performance aspects of glass fiber insulation on the outside of basement walls*. Symposium on Thermal Insulation Performance, Tampa, Fla., ASTM Special Technical Publication, Vol. 718, 1980, pp. 77-91.

Bomberg, M.T. 1980. *Some performance aspects of glass fiber insulation on the outside of basement walls*. Symposium on Thermal Insulation Performance, Tampa, Fla., 1978. ASTM Special Technical Publication, Vol. 718, 1980, pp. 77-91.

Bomberg M.T., and M.K. Kumaran. 1994. Laboratory and roofing exposures of cellular plastic insulation to verify a model of aging. *Roofing Research and Standards Development, ASTM STP 1224*, T. J. Wallace and W. J. Rossiter, Jr., eds. Philadelphia, Pa.: American Society for Testing and Materials.

Bomberg M.T., Y.S. Muzychka, D.G. Stevens, and M.K. Kumaran. 1994. A comparative test method to determine thermal resistance under field conditions. *J. Thermal Insulation and Building Envelopes*, Vol. 18.

Crocker, C.R. 1961. House basements. *Canadian Building Digest* (13). Ottawa, Ontario: National Research Council of Canada, Division of Building Research.

Crocker, C.R. 1974. Example result: Moisture and thermal considerations in basement walls. *Canadian Building Digest* (161). Ottawa, Ontario: National Research Council of Canada, Division of Building Research.

Elmorth, A., and I. Holglund. 1971. *New basement wall designs for below-grade living space*. Originally published in Stockholm, 1971. Technical translation prepared for National Research Council, Division of Building Research, Ottawa, 1975.

Hutcheon, N.B. 1963. Requirements for exterior walls. *Canadian Building Digest* (48). Ottawa, Ontario: National Research Council of Canada, Division of Building Research.

Maref, W., M.C. Swinton, M.K. Kumaran, and M.T. Bomberg. 2001. 3-D analysis of thermal resistance of exterior basement insulation systems (EIBS). J*ournal of Building and Environment* 36 (4): 407-419.

Muzychka Y. 1992. A method to estimate thermal resistance under field conditions. NRC/IRC internal report No 638.

Nelson, B.D. 1989. Conditions of a sample of Minnesota exterior foundation wall insulation materials. *Thermal Performance of the Exterior Envelopes of Buildings IV.* Atlanta: American Society of Heating, Refrigerating and Air-Conditioning Engineers, Inc.

Sterling, R.L. 1986. Moisture absorption and its effect on the thermal properties of EPS insulation for foundation applications. Contract report by Underground Space Center, University of Minnesota, October, 1996.

Swinton M.C., M.T. Bomberg, M.K. Kumaran, and W. Maref. 1999. In situ Performance of Expanded Polystyrene in the Exterior Basement Systems (EIBS). *Journal of Thermal Envelopes & Building Sci.* Vol. 23.

Tao, S.S., M.T. Bomberg, and J.J. Hamilton. 1980. *Glass fiber as insulation and drainage layer on exterior of basement walls.* Symposium on Thermal Insulation Performance, Tampa, Fla., 1978, pp. 57-76. ASTM Special Technical Publication, Vol. 718 (NRCC-19317).

Timusk, J. 1981. Insulation retrofit of masonry basements. Report for the Ministry of Municipal Affairs and Housing, Ontario, ISBN 0-7743-7052-1.